International Journal of Nanomedicine

Dovepress
open access to scientific and medical research

Open Access Full Text Article

ORIGINAL RESEARCH

RGD- and VEGF-Mimetic Peptide Epitope-Functionalized Self-Assembling Peptide Hydrogels Promote Dentin-Pulp Complex Regeneration

This article was published in the following Dove Press journal:
International Journal of Nanomedicine

International Journal of Nanomedicine downloaded from https://www.dovepress.com/
For personal use only.

Kun Xia[1,2,*]
Zhuo Chen[3,4,*]
Jie Chen[1]
Huaxing Xu[1]
Yunfei Xu[1]
Ting Yang[1]
Qi Zhang[1]

[1]Department of Endodontics, School and Hospital of Stomatology, Tongji University, Shanghai Engineering Research Center of Tooth Restoration and Regeneration, Shanghai 200072, People's Republic of China; [2]Department of Preventive Dentistry, School and Hospital of Stomatology, Wenzhou Medical University, Wenzhou 325027, People's Republic of China; [3]Department of Endodontics, The Affiliated Stomatology Hospital, Zhejiang University School of Medicine, Hangzhou 310006, People's Republic of China; [4]Key Laboratory of Oral Biomedical Research of Zhejiang Province, Zhejiang University School of Stomatology, Hangzhou 310006, People's Republic of China

*These authors contributed equally to this work

Correspondence: Qi Zhang
Department of Endodontics, School and Hospital of Stomatology, Tongji University, Shanghai, Engineering Research Center of Tooth Restoration and Regeneration, Yanchang Road 399, Shanghai 200072, People's Republic of China
Tel +86-21-66311659
Fax +86-21-66524025
Email qizhang@tongji.edu.cn

Introduction: Cell-based tissue engineering is a promising method for dentin-pulp complex (DPC) regeneration. The challenges associated with DPC regeneration include the generation of a suitable microenvironment that facilitates the complete odontogenic differentiation of dental pulp stem cells (DPSCs) and the rapid induction of angiogenesis. Thus, the survival and subsequent differentiation of DPSCs are limited. Extracellular matrix (ECM)-like biomimetic hydrogels composed of self-assembling peptides (SAPs) were developed to provide an appropriate microenvironment for DPSCs. For functional DPC regeneration, the most important considerations are to provide an environment that promotes the adequate attachment of DPSCs and rapid vascularization of the regenerating pulp. Morphogenic signals in the form of growth factors (GFs) have been incorporated into SAPs to promote productive DPSC behaviors. However, the use of GFs has several drawbacks. We envision using a scaffold with SAPs coupled with long-term factors to increase DPSC attachment and vascularization as a method to address this challenge.

Methods: In this study, we developed synthetic material for an SAP-based scaffold with RGD- and vascular endothelial growth factor (VEGF)-mimetic peptide epitopes with the dual functions of dentin and pulp regeneration. DPSCs and human umbilical vein endothelial cells (HUVECs) were used to evaluate the biological effects of SAP-based scaffolds. Furthermore, the pulpotomized molar rat model was employed to test the reparative and regenerative effects of SAP-based scaffolds.

Results: This scaffold simultaneously presented RGD- and VEGF-mimetic peptide epitopes and provided a 3D microenvironment for DPSCs. DPSCs grown on this composite scaffold exhibited significantly improved survival and angiogenic and odontogenic differentiation in the multifunctionalized group in vitro. Histological and functional evaluations of a partially pulpotomized rat model revealed that the multifunctionalized scaffold was superior to other options with respect to stimulating pulp recovery and dentin regeneration in vivo.

Conclusion: Based on our data obtained with the functionalized SAP scaffold, a 3D microenvironment that supports stem cell adhesion and angiogenesis was generated that has great potential for dental pulp tissue engineering and regeneration.

Keywords: dentin-pulp complex regeneration, dental pulp stem cells, self-assembling peptides, cell adhesion, angiogenesis, multifunctionalization

Introduction

Cell-based tissue engineering is a promising method for dentin-pulp complex (DPC) regeneration that utilizes a combination of stem cells, scaffolds and growth factors

© 2020 Xia et al. This work is published and licensed by Dove Medical Press Limited. The full terms of this license are available at https://www.dovepress.com/terms.php and incorporate the Creative Commons Attribution – Non Commercial (unported, v3.0) License (http://creativecommons.org/licenses/by-nc/3.0/). By accessing the work you hereby accept the Terms. Non-commercial uses of the work are permitted without any further permission from Dove Medical Press Limited, provided the work is properly attributed. For permission for commercial use of this work, please see paragraphs 4.2 and 5 of our Terms (https://www.dovepress.com/terms.php).

(GFs).[1,2] Stem cell niches are 3-D microenvironments composed of crosslinked networks of extracellular matrix (ECM) proteins, oxygen, nutrients and GFs.[3,4] However, two notable limitations in the current DPC regeneration protocol have been identified. (1) The newly formed "dentin-like" bridge is usually fragmented and permeable, resulting in bacterial recontamination. This limitation originates from the fact that currently available biomaterials are unable to provide adequate attachment and induce mineralization in dental pulp stem cells (DPSCs). (2) The second limitation is pulp tissue necrosis due to the compromised blood supply in the exposed axial wall. This limitation derives from the lack of effective and quick vascularization for DPSCs in the dental pulp. One approach to overcome this problem is to functionalize scaffolds that induce cell adhesion, promote cell survival, and provide morphogenic signals for angiogenesis and odontogenesis to DPSCs.[4,5] ECM not only provides structural support but also regulates cellular functions, such as cell adhesion, proliferation and differentiation. Moreover, the ECM modulates the signal transduction pathways activated by various bioactive molecules, such as GFs and cytokines. Because of its versatile properties, ECM-like scaffolds have been widely explored for applications in tissue engineering and regenerative medicine. Subsequent research has explored numerous strategies to develop and synthesize ECM-like biomimetic materials to provide an appropriate microenvironment for DPSCs.[6–8] For this purpose, ECM-like biomimetic scaffolds must be developed and synthesized to provide an appropriate microenvironment for DPSC engraftment and/or host-cell ingrowth.

Recently, self-assembling peptides (SAPs) have been shown to be unique biomaterials for 3D cell culture and excellent candidate scaffolds for both soft and mineralized dental tissues in tissue engineering.[9,10] SAPs are an example of a smart material that can be modified to create customized matrices with structures very similar to natural ECM.[11] The SAP RADA16 (Ac-RADARADARADA RADA-NH_2, RAD), which is one type of injectable SAP, has been increasingly investigated as a tailorable biomimetic material for facilitating tissue engineering.[12,13] In addition, multifunctionalized scaffolds for multiple targets have been obtained by combining multiple functional motifs with identical self-assembling backbone sequences prior to self-assembly.[14–18] Since these hydrogel systems are highly biocompatible, many of these approaches aim to incorporate morphogenetic proteins (such as fibroblast growth factor-2, vascular endothelial growth factor (VEGF), transforming growth factor-β, and bone morphogenetic proteins, among others) into SAPs to guide DPSC responses.[19–22] Notably, these signals are typically proteins with a short half-life, and the controlled release and degradation of these proteins remains a challenge.[23] Thus, the emphasis has shifted to biomaterials that are able to be coupled with GFs to achieve long- term effects.

Previous studies have identified the most important properties that should be considered in developing SAPs are to provide for the adequate attachment of DPSCs and rapid vascularization of the regenerating pulp.[4,5,24] We envision an ideal scaffold with SAPs coupled with long-term factors to increase DPSC attachment and vascularization as a method to address this challenge. In particular, various bioactive short peptide motifs function as analogs of soluble GFs.[18] The designer SAP PRG was developed to provide binding motifs for integrins by directly coupling a 2-unit RGD binding sequence to RAD.[17] The functionalized SAP RAD/PRG has been proven to promote the adhesion, proliferation and differentiation of MC3T3-E1 cells,[17] degenerated nucleus pulposus cells[25] and periodontal ligament fibroblasts.[26] KLT, a motif that reproduces amino acids 17–25 in the helical region of VEGF that binds to RAD, binds to and activates VEGF receptors.[27,28] The functionalized SAP RAD/KLT has been shown to exert distinct angiogenic activities in vitro and in vivo.[27,28] Moreover, RAD maintains the viability of and supports the odontoblastic differentiation of dental pulp-derived stem cells.[29,30] Based on these results, PRG and KLT are ideal substrates for DPC regeneration, which requires both the cell adhesion capability and angiogenesis. Therefore, we hypothesized that SAPs that incorporate these two unique functional motifs, PRG and KLT, will form an ideal scaffold to promote the long-term survival of DPSCs and concurrently achieve adequate attachment, rapid vascularization and appropriate mineralization during DPC regeneration.

In the present study, we designed a simple single-step strategy and procedure to incorporate cell adhesion-promoting and angiogenic motifs into an RAD scaffold, thereby addressing the central considerations by not only providing an injectable and 3D nanofibrous structure but also promoting cell adhesion, angiogenesis and mineralization. Thus, the aims of this study were: (1) to design and synthesize a multifunctional RAD/PRG/KLT SAP scaffold with the appropriate 3D structure and desirable cell adhesion and angiogenesis characteristics, (2) to assess the survival and differentiation of DPSCs within this scaffold, and (3) to

investigate the application of this scaffold in promoting DPC regeneration in partially pulpotomized rat molars in vivo.

Materials and Methods

Peptide Synthesis and Sample Preparation

The RAD solution (1% w/v, 10 mg mL^{-1}) was purchased as PuraMatrix™ from BD Biosciences (Bedford, MA). The two functional peptides PRG and KLT were custom-synthesized by ChinaPeptides Co., Ltd (purity >95%, Shanghai, China). The peptide sequences and descriptions are listed in Table 1. The proportions chosen for the peptides were determined according to the results of previous studies.[15,16] The self-assembling peptide solutions were prepared according to a previously reported protocol.[31–33] Briefly, the peptide powders were dissolved in distilled water at a concentration of 1% (w/v), sonicated for 30 min and filter-sterilized with an Acrodisc Syringe Filter (0.2 μm HT Tuffrun membrane, Pall Corp., Ann Arbor, MI) prior to use. The functional peptide solutions were mixed with 1% RAD solution at a volume ratio of 1:1 to obtain the functionalized peptide mixtures (RAD/PRG and RAD/KLT). Then, the RAD/PRG and RAD/KLT solutions were mixed at a ratio of 1:1 to form the combined solution, namely, RAD/PRG/KLT. Figure 1A shows the amino acid sequences and molecular models of RAD, PRG and KLT; Figure 1B shows the proposed molecular models for RAD/PRG and RAD/KLT. Figure 1C shows a schematic illustrating the nanofibrous RAD/PRG/KLT scaffold hydrogel. The typical AFM morphology of the RAD/PRG/KLT solution and SEM morphology of the RAD/PRG/KLT scaffold hydrogel are also presented in Figure 1D.

Table 1 Functionalized SAP Scaffolds Used in This Study

Name	Sequences	Description
RAD	Ac-$(RADA)_4$-NH_2	Self-assembling peptide
PRG[18]	Ac-$(RADA)_4$GPRGDSGYRGDS-NH_2	RGD-mimicking peptide: 2-unit RGD motifs
KLT[26]	Ac-$(RADA)_4G_4$KLTWQELYQLKYKGI-NH_2	VEGF-mimicking peptide: reproducing the 17–25 helix region of VEGF
RAD/PRG RAD/KLT	– –	50%RAD+50%PRG 50%RAD+50%KLT
RAD/PRG/KLT	–	50%RAD+25%RAD/PRG+25%RAD/KLT

Circular Dichroism (CD) Spectroscopy

CD spectra were collected using a MOS-500 spectrometer (Bio-Logic, France). A quartz cuvette with a 1 mm path length was used for the measurements. Far-UV CD spectra were recorded from 185 to 265 nm. The samples were diluted to a working concentration of 0.01% w/v. Then, the samples were incubated at room temperature overnight and the spectra were recorded 3 times.

Fourier Transform Infrared (FTIR) Spectroscopy

A Nicolet iS50 FTIR spectrometer (Thermo Fisher, Madison, USA) was used to obtain the FTIR spectra. The concentrations of RAD/PRG, RAD/KLT, and the RAD/PRG/KLT combination were 2% (w/v). The samples were prepared in D_2O at least 12 hours before the measurement. The spectra were collected at wavelengths ranging from 1700–1600 cm^{-1} at a 1 cm^{-1} resolution and smoothed using the Savitsky-Golay function after buffer subtraction. The spectra were recorded as the absorbance values at each data point in triplicate.

Atomic Force Microscopy (AFM)

AFM imaging was performed on an atomic force microscope (Bruker Dimension ICON, Billerica, MA, USA) in tapping mode. All of the peptide solutions (RAD/PRG, RAD/KLT, and RAD/PRG/KLT) were diluted to a working concentration of 0.01% (w/v). Then, 5 μL of each diluted sample were added dropwise to a freshly cleaved mica surface, air-dried and subjected to the AFM analysis. Images of the samples were acquired using a silicon scanning probe with a resonance frequency of 75 kHz, a spring constant of 2.8 N/m, a tip curvature radius of 10 nm and a length of 225 μm.

Preparation of DPSCs

Local ethical approval was granted by the Medical Ethics Committee, Faculty of Dentistry, Tongji University, Shanghai, China. hDPSCs were isolated from extracted premolars and third molars without caries or periodontal diseases. Informed consent was obtained from patients aged 18–25 years. Human umbilical vein endothelial cells (HUVECs) were obtained from the Chinese Academy of Sciences (category number: EAhy926). Rat DPSCs (rDPSCs) were isolated from the lower incisors of 3-week-old male Sprague-Dawley rats (weighing 90–110 g).

The "stemness" of the freshly isolated DPSCs was assessed by performing a flow cytometry analysis of the

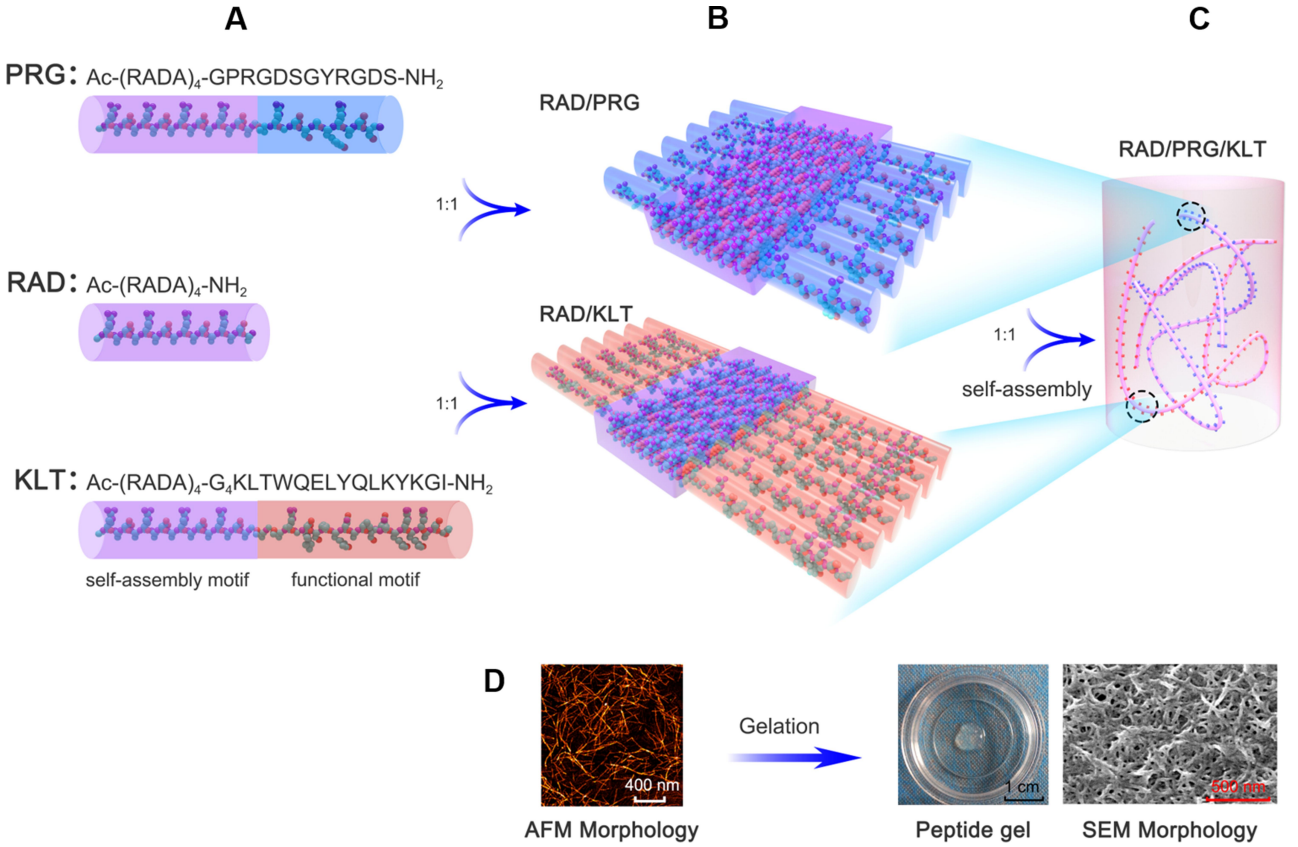

Figure 1 Molecular model and schematic illustration of the functionalized peptide scaffold RAD/PRG/KLT. (**A**) Amino acid sequences and molecular models of RAD, PRG and KLT. (**B**) Proposed molecular models for RAD/PRG and RAD/KLT. (**C**) Schematic illustration of the RAD/PRG/KLT hydrogel. (**D**) The typical AFM morphology of the RAD/PRG/KLT solution and SEM morphology of the RAD/PRG/KLT gel are presented.

expression of the mesenchymal stem cell markers CD34-PE, CD105-APC (BD Bioscience), CD45-PE and CD90-PE (R&D Systems). Furthermore, the multilineage differentiation capacity of the DPSCs was confirmed by performing alizarin red S, alcian blue and oil red O staining to identify the osteogenic, chondrogenic, and adipogenic differentiation properties, respectively, using previously described methods.[34]

Hydrogel Formation

Transwell inserts (Millipore, MA) were used for peptide gel formation. Briefly, the inserts were placed in a 24-well culture plate with 400 μL of cell culture medium (alpha-modified Eagle's medium (α-MEM)) in each well. Then, 100 μL of the functional SAP solution were added to the insert, and 400 mL of culture medium were gently loaded onto the solution, followed by an incubation of the plate at 37 °C for 1 hour to allow gelation. Subsequently, the medium was carefully aspirated and then changed twice to remove any free acid residues remaining from peptide synthesis.

3D Cell Culture in Self-Assembling Peptide Scaffolds

hDPSCs were encapsulated in SAP-based hydrogels at a concentration of 0.25% (w/v) as previously reported.[15] Briefly, after digestion in the culture dish and centrifugation, the hDPSCs were suspended in 10% (w/v) sucrose at twice the final desired cell density (2×10^6 cells/mL). The peptide solution was prepared by diluting the stock with sterile 20% sucrose to generate a 2× concentration of peptide in 10% sucrose. Subsequently, 50 μL of the 2× cell suspension and 50 μL of the 2× peptide solution were mixed and then carefully added to the Transwell inserts. Gelation was initiated by gently adding culture medium on top of the mixture. The culture medium was changed at least twice to equilibrate the pH. hDPSCs cultured in tissue culture plates (TCPs) were used as controls.

Scanning Electron Microscopy (SEM)

After gelation, peptide hydrogels (alone or with cells seeded inside) were fixed with 2.5% glutaraldehyde,

dehydrated with successive ethanol washes, and dried using a CO_2 critical point dryer (Samdri-PVT-3D; Tousimis, Rockville, MD, U.S.A.). Then, the samples were coated with platinum and images were captured using SEM (JEOL) at a voltage of 20 kV.

Rheology

The rheological measurements of the peptide samples were performed using a RheoStress AR G2 instrument (TA Instruments, Inc., U.S.A.). One milliliter of each 1% (w/v) peptide solution (RAD/PRG, RAD/KLT, and RAD/PRG/KLT) was mixed with 500 μL of α-MEM at a volume ratio of 2:1. The sample was incubated for 3 min and then loaded onto the lower plate of the rheometer (α-MEM was added to induce the peptide in solution to form hydrogel). During this process, strain sweeps between the storage (elastic) modulus (G′) and loss (viscous) modulus (G″) of the peptides were recorded at frequencies ranging from 0.1 rad/s to 100 rad/s and a constant shear stress of 1 Pa at 37 °C. Data acquisition was repeated in triplicate.

Cell Adhesion and Morphology

The attachment of the cells to scaffolds and cell morphology were observed using immunofluorescence staining (IF) or SEM (described above). SAP-based hydrogels were prepared as described above. DPSCs were seeded on the surface of hydrogels (2×10^4 cells per well, n=3). After 3 days, the cells were fixed with 4% paraformaldehyde (PFA) for 15 min and permeabilized with 0.1% Triton X-100 for 5 min at room temperature. Fluorescent phalloidin and DAPI (Sigma) were used to label F-actin and nuclei, respectively. The images were captured using a Leica TCS SP5 II confocal microscope (Leica Microsystems, Wetzlar, Germany).

Cell Viability Assay

hDPSCs were encapsulated in SAP-based hydrogels as described above. In accordance with the manufacturer's instructions, a live/dead viability/cytotoxicity assay kit (Invitrogen) was used to stain hDPSCs that had been cultured for 3 days. Fluorescence was analyzed using a Leica TCS SP5 II confocal microscope (Leica Microsystems).

Cell Proliferation Assay

The proliferation of hDPSCs on various hydrogels was evaluated. hDPSCs were encapsulated in SAP-based hydrogels in a 96-well plate as described above. After 1, 4 and 7 days, the number of cells was evaluated using cell counting kit-8 reagents (CCK-8, Dojindo, Japan). The absorbance was measured at 450 nm using a microplate reader (Bio-Tek, Hercules).

Odontogenic Differentiation Assay and ALP Staining

The odontogenic differentiation of encapsulated hDPSCs (described above) was induced using culture medium supplemented with 10 mM sodium β-glycerophosphate (Sigma-Aldrich), 10 nM dexamethasone (Sigma-Aldrich) and 50 μg/mL ascorbic acid (Sigma-Aldrich) for 21 days.

The hDPSCs/hydrogels were fixed, stained with the Alkaline Phosphatase Color Development Kit (Beyotime Biotechnology) and then analyzed using an inverted microscope (Nikon Eclipse 80i).

Enzyme-Linked Immunosorbent Assay (ELISA)

hDPSCs were encapsulated in SAP-based hydrogels in 48-well plates as described above. After 1, 3, 7 and 14 days, the culture medium was collected, and the total amount of VEGF that had been secreted by the hDPSCs in the hydrogels was analyzed by using ELISA kits according to the manufacturer's protocols (R&D System).

Quantitative Real-Time PCR (RT-qPCR) Analysis of Gene Expression

hDPSCs were encapsulated in SAP-based hydrogels in 48-well plates as described above. After odontogenic differentiation as described above, the hDPSCs/hydrogels were disrupted mechanically and collected for an analysis of odontogenesis-related gene expression. After 14 days of culture, the hDPSCs/hydrogels were disrupted mechanically and collected for the analysis of angiogenesis-related gene expression. The total RNA was extracted using TRIzol reagent (Invitrogen) according to the manufacturer's instructions. Then, cDNAs were reverse transcribed from the total RNA using a reverse transcriptase (Roche). After the cDNAs were acquired, the expression levels of odontogenesis-related genes (*ALP*, *DMP1* and *DSPP*) and angiogenesis-related genes (*VEGFA*, *vWF*, *CD31* and *Ang-1*) were analyzed using RT-qPCR, with the *GAPDH* housekeeping gene serving as a control. The primers (Sango Biotech, Shanghai, China) used to amplify all genes are shown in Table 2. A FastStart Essential DNA Green Master kit (Roche) and a Light Cycler 96 instrument (Roche) were used for the RT-qPCR analysis.

Table 2 Primers for RT-qPCR

Genes	Forward Primer 5′-3′	Reverse Primer 5′-3′
Human GAPDH	GAAGGTCGGAGTCAACGG	GGAAGATGGTGATGGGATT
Human ALP	ATG GTG GAC TGC TCA CAA C	GAC GTA GTT CTG CTC GTG GA
Human DMP1	TTCCTCTTTGAGAACATCAACCTG	ACTCACTGCTCTCCAAGGGT
Human DSPP	AAAGTGGTGTCCTGGTGCAT	CCTGGATGCCATTTGCTGTG
Human VEGF	AGGGCAGAATCATCACGAAGT	AGGGTCTCGATTGGATGGC
Human CD31	CCAAGCCCGAACTGGAATCT	CACTGTCCGACTTTGAGGCT
Human Ang-1	TCGTGAGAGTACGACAGACCA	TCTCCGACTTCATGTTTTCCAC
Human vWF	GAGCTGCGAGGAGAGGAATC	AGTCTTCAGGGTCAACGCAG

Angiogenesis-Inducing Activity of hDPSCs/SAP-Conditioned Medium (CM)

The proliferation, migration and tube formation of HUVECs cultured with CM were examined to determine the ability of the SAPs to induce proangiogenic capability of hDPSCs. CM was prepared from 50% culture medium mixed with 50% supernatant harvested from hDPSCs/SAP 3D cultures, as described above, on the 7th day. Both CM prepared from the supernatant of hDPSCs that had been 2D-cultured in TCPs and α-MEM cell culture medium served as controls. After 1, 4, and 7 days of culture with CM, the proliferation of HUVECs was analyzed with the CCK-8 reagent (Dojindo, Japan).

Cell migration was analyzed using scratch and Transwell assays. After a scratch was generated in a confluent monolayer, HUVECs were incubated with CM for 6 hours and the migration rate of the cells was calculated as the fold change in the area relative to the initial area. Seven hundred fifty microliters of CM were added to the wells, and HUVECs (2×10^4 cells) in 200 μL of culture medium were seeded into the inserts. After a 12 hour incubation, the cells that had passed through the insert membranes were fixed, stained and analyzed.

Matrigel matrix (50 μL, BD Biosciences) was poured into the wells of a 96-well culture plate and allowed to solidify (37 °C, 30 min). HUVECs (3×10^4 cells/well) were seeded on the gel and cultured with CM. After a 6 hour incubation, tube formation was observed and quantified.

Experimental Animals and Partially Pulpotomized Molar Models

Thirty-five 8-week-old male Sprague-Dawley rats (weighing 230–260 g) were used in this experiment. They were purchased from the Central Lab of Tongji University Laboratory Animal Center (Shanghai, China) and maintained in a conventional environment in the Tongji University Animal Facility according to institutional guidelines. All the experimental procedures were approved by the Animal Welfare Committee of Tongji University (TJLAC-017-043).

The rats were anesthetized with pentobarbital sodium (100 mg/kg) via an intraperitoneal injection. The rats were randomly divided into 7 groups (n = 5 animals per group). In groups 1 through 6, the dental pulp under the occlusal surface of the left upper first molar was exposed and partially pulpotomized using a no. 1/4 round bur under a guide plate, followed by irrigation and drying. Then, the residual pulp was implanted with one of the mixtures described in Table 3. The cavities were sealed with mineral trioxide aggregate (MTA) (Henry Schein) and self-adhesive flowable resin composite

Table 3 Rat Groups and the Materials Implanted on Residual Pulp in the Different Groups

Group Number	Group Name	Description		
		10% Sucrose (μL)	rDPSCs	Peptide Solution (μL)
1	Sucrose	1	0	0
2	Sucrose+ rDPSC	1	2.0×10^4	0
3	RAD+ rDPSC	0.5	2.0×10^4	0.5 RAD
4	RAD/PRG+ rDPSC	0.5	2.0×10^4	0.5 RAD/PRG
5	RAD/KLT+ rDPSC	0.5	2.0×10^4	0.5 RAD/KLT
6	RAD/PRG/KLT+ rDPSC	0.5	2.0×10^4	0.5 RAD/PRG/KLT
7	Normal control	0	0	0

(Dyad Flow, KaVo) according to the manufacturers' instructions. The rats in group 7, which did not undergo any operation, were used as the normal control group. Twenty-eight days after the dental procedures, the animals were anesthetized, perfused and immersed in 4% paraformaldehyde.

Histological Analysis

After fixation, the maxillae were dissected and demineralized in 10% ethylenediaminetetraacetic acid (EDTA) for 8 weeks. Then, the specimens were processed, embedded in paraffin, and sectioned into 4 μm sections. Hematoxylin and eosin (H&E) staining was performed using standard protocols. The criteria used to assess the specimens were consistent with the method described by Koliniotou-Koumpia and Tziafas.[35] Scores were recorded for inflammatory cell infiltration, tissue necrosis, and the thickness of hard tissue formation. In addition, the differences of ratios of the coronal pulp, the thickness and the porosity of dental bridges among groups were compared and analyzed.

Immunohistochemical (IHC) Staining

IHC staining was performed as previously described.[36] Briefly, after endogenous peroxidase activity had been blocked, sections were blocked with serum and then incubated with a primary antibody against DMP1-C-8G10.3 (1:300; gift from Dr. Chunlin Qin, TA&M University, College of Dentistry) or CD31 (1:500; Abcam) according to the manufacturers' recommendations. Following an incubation with biotin-labeled secondary antibodies (1:1000, Abcam), streptavidin-peroxidase and a DAB Detection Kit (Streptavidin-Biotin, MXB) were used for visualization. Sections were mounted and imaged with a Nikon Eclipse 80i microscope.

Statistical Analysis

Data were statistically analyzed using SPSS 20 software and are presented as means ± standard errors of the means (SEM). Between-group comparisons were analyzed using one-way analysis of variance (ANOVA) with Tukey's test. $P<0.05$ was accepted as statistically significant.

Results

Structural and Mechanical Properties of the SAPs

The secondary structures and morphology of the SAPs were assessed in this study. CD and FITR spectroscopy were used to determine the secondary structures of the SAPs. Spectra typical of β-sheet structures were obtained for all peptide solutions, with a positive maximum band at 195 nm and a negative maximum band at 216 nm. The intensities of the CD spectra of the RAD/PRG/KLT solutions were decreased compared with the RAD, RAD/PRG and RAD/KLT solutions (Figure 2A). The secondary structures were further investigated using FTIR spectroscopy. The most informative region regarding the secondary structure of proteins was the amide I region between wavenumbers 1700 and 1600 cm^{-1}. Consistent with the CD results, the strong absorption peaks at approximately 1635 cm^{-1} in the RAD/PRG/KLT spectra were decreased compared with the RAD, RAD/PRG and RAD/KLT spectra (Figure 2B).

AFM was employed to observe the surface structures of the SAPs. The self-assembly process successfully occurred in the functional peptide mixtures (Figure 2C). The average diameters of the nanofibers assembled from RAD, RAD/PRG, RAD/KLT and RAD/PRG/KLT were 13.1 ± 1.2, 17.0 ± 2.3, 16.3 ± 1.4 and 17.9 ± 1.3 nm, respectively, consistent with the number of amino acids in the peptides. The diameters of nanofibers assembled from the functionalized peptide mixtures were thicker than pure RAD (Figure 2D). After adding cell culture medium (α-MEM), the SAP-based solutions self-assembled to form transparent hydrogels (Figure 2E). SEM images also confirmed that all peptides formed nanofibers, and the nanofibers further interweaved to form porous structures (Figure 2F).

Furthermore, a rotational rheometer was used to investigate the mechanical properties of the SAP-based hydrogels. The frequency sweep results (Figure 2G) obtained at 37 °C revealed a similar viscoelasticity of the 4 hydrogels (including the storage modulus G′ and the loss modulus G″), and both G′ and G″ were independent of the shear rate frequency. The 4 samples exhibited G′ >G″ (Figure 2H), indicating that the SAPs had certain elastic properties despite their good fluidity, and further suggesting that the addition of the functionalized motifs did not interfere with the gel-forming ability of RAD. In addition, the values of G′ and G″ for RAD/PRG/KLT were greater than the other 3 functionalized SAPs in the range of the shear rate frequencies (Figure 2I), whereas the values for G′ and G″ of the 3 functionalized SAPs were similar, indicating that the stiffness of the RAD/PRG/KLT hydrogels was greater than the other 3 peptide hydrogels.

Effects of the SAPs on hDPSCs

Once the functionalized SAPs were successfully self-assembled, we explored the bioactivity of these SAPs in the presence of hDPSCs. Prior to this experiment, we

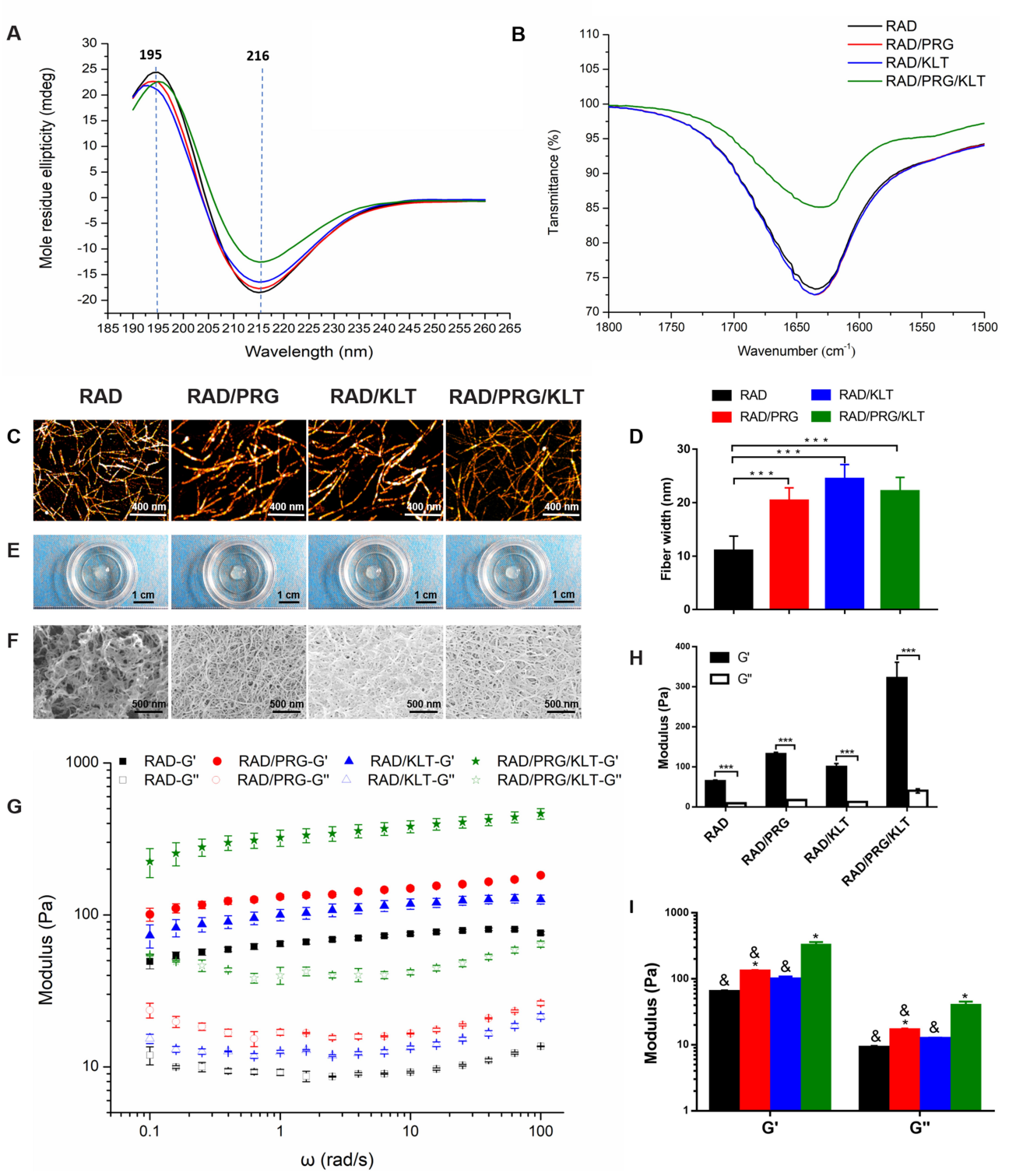

Figure 2 Microstructural, morphological and rheological studies of the SAPs. (**A**) CD spectra of the SAPs. (**B**) FTIR spectra of the SAPs. (**C**) AFM images of the SAPs. (**D**) Average fiber width of the SAPs. (**E**) The SAPs self-assembled to form hydrogels in vitro. (**F**) SEM images of the SAPs. (**G**) Rheological analysis of the SAPs. (**H**) G′ and G″ of the SAPs. (**I**) Differences of G′ and G″ among the SAPs. Values are represented as means ± SD. The following symbols indicate significant differences ($P < 0.05$): *Compared to RAD; [&]Compared to RAD/PRG/KLT. ***$P < 0.001$.

characterized the "stemness" of the freshly isolated cells. The results of the flow cytometry showed positivity for CD105 and CD90 and negativity for CD34 and CD45, which confirmed the mesenchymal stem cell lineage of the isolated cells (Figure S1). In addition, these cells underwent osteogenic, adipogenic and chondrogenic differentiation after culture

with the relevant induction media for a period of 3 weeks (Figure S1).

First, we evaluated the biocompatibility of the functionalized SAPs. The viability of hDPSCs in 3D-culture in the SAP hydrogel scaffolds was determined using the live/dead cell viability assay. As shown in Figure 3A, the survival rate of hDPSCs cultured in each of the 3D SAP hydrogel scaffolds was greater than 90% after 7 days. Thus, the addition of functional motifs to the RAD backbone did not increase the cytotoxicity toward the hDPSCs compared to pure RAD (Figure 3B, $P > 0.05$).

Next, the attachment of the hDPSCs to scaffolds, which is essential for their subsequent survival and differentiation, was assessed. The hDPSCs were uniformly encapsulated in hydrogels and displayed similar morphologies in the RAD and functionalized SAP hydrogels (Figure 3C). Specifically, the hDPSCs spread throughout the hydrogels at all depths, suggesting that the hydrogel scaffolds provided a suitable 3D culture environment for hDPSCs in all groups. The spread morphology of a single cell is displayed in the inserted image (Figure 3C). In addition, SEM images showed that the hDPSCs were embedded in the scaffolds and tightly attached to the nanofibers via many extended pseudopodia after 3 days of 3D culture in SAP hydrogel scaffolds (Figure 3D).

Then, the proliferation of the hDPSCs cultured in 3D scaffolds was quantitatively detected. As shown in Figure 3E, the number of cells in each scaffold increased over time. The proliferation rate of hDPSCs cultured in functionalized SAP scaffolds was obviously higher than cells cultured in the RAD scaffold after 7 days ($P<0.0001$). Moreover, the number of hDPSCs cultured in RAD/PRG and RAD/PRG/KLT hydrogels was significantly greater than the number of cells cultured in RAD/KLT hydrogels ($P<0.05$). However, an obvious difference was not observed between the RAD/PRG and RAD/PRG/KLT groups ($P>0.05$).

Finally, the odontoblastic differentiation and proangiogenic capability of hDPSCs cultured in 3D scaffolds was detected. Odontoblastic differentiation was observed by performing ALP staining of the mineral nodules (Figure 3F) and examining the expression of odontogenesis-related genes on day 14 after induction. ALP-positive areas of hDPSCs cultured in the 3D RAD/PRG/KLT scaffold were significantly larger than the other groups (Figure 3G). The RT-qPCR results showed significantly increased expression of ALP, DMP1 and DSPP in the hDPSCs from the RAD/PRG/KLT group at 14 days ($P<0.05$) (Figure 3H).

The proangiogenic capability of hDPSCs was partially determined by assessing angiogenesis-related gene expression and the ability of the hDPSC/SAP construct to secrete VEGF. The RT-qPCR results showed significantly increased expression of VEGF, CD31, Ang-1 and vWF in hDPSCs from the RAD/KLT and RAD/PRG/KLT groups at 14 days ($P<0.05$), but no obvious differences were detected between the two groups ($P>0.05$) (Figure 3I). The ELISA results revealed a significantly greater amount of VEGF that was secreted by hDPSCs in the RAD/KLT and RAD/PRG/KLT groups ($P<0.05$), but no obvious differences were detected between these two groups ($P>0.05$) (Figure 3J). The gene and protein levels were similar.

Effects of hDPSCs/SAPs on HUVECs

Endothelial cells are cell types essential for angiogenesis. The proliferation (Figure 4A), horizontal (Figure 4B) and vertical migration (Figure 4D) and tube formation (Figure 4F) of HUVECs cultured with hDPSC/SAP-CM were studied to further evaluate the proangiogenic capability of hDPSCs cultured in 3D scaffolds. HUVECs cultured with the CM of RAD/PRG/KLT+hDPSCs significantly differed from HUVECs from the other groups (Figure 4A, C, E, and G) ($P<0.05$). The results of all the assays described above were consistent.

Histological and IHC Staining After Transplantation

A partially pulpotomized rat molar model was used to investigate the effects of SAPs on regeneration, and the histology was evaluated using H&E staining (Figure 5A–G). After 28 days, a normal organization of radicular pulp tissue without tissue necrosis was observed in all groups. Substantial inflammatory cell infiltration was observed in the sucrose group, whereas few inflammatory cells infiltrated in the other groups. Notably, the inflammatory cells were confined to a region just below the reparative dental bridges in the RAD/PRG/KLT +rDPSC group but were scattered in the other groups. The formation of dentin bridges varied among the groups. The dentin bridges in the sucrose group showed bone-like tissues, whereas sealing of the exposure site was not observed in the sucrose+rDPSC group. The RAD+rDPSC group showed scattered and sparse calcification without dentin bridges. In the RAD/PRG+rDPSC and RAD/KLT+rDPSC groups, the bridge-like structures were incomplete, and the pulp tissue was connected to the outside. In particular, intact dentin bridges and well-aligned odontoblast-like cell layers were observed in the RAD/PRG/KLT+rDPSC group.

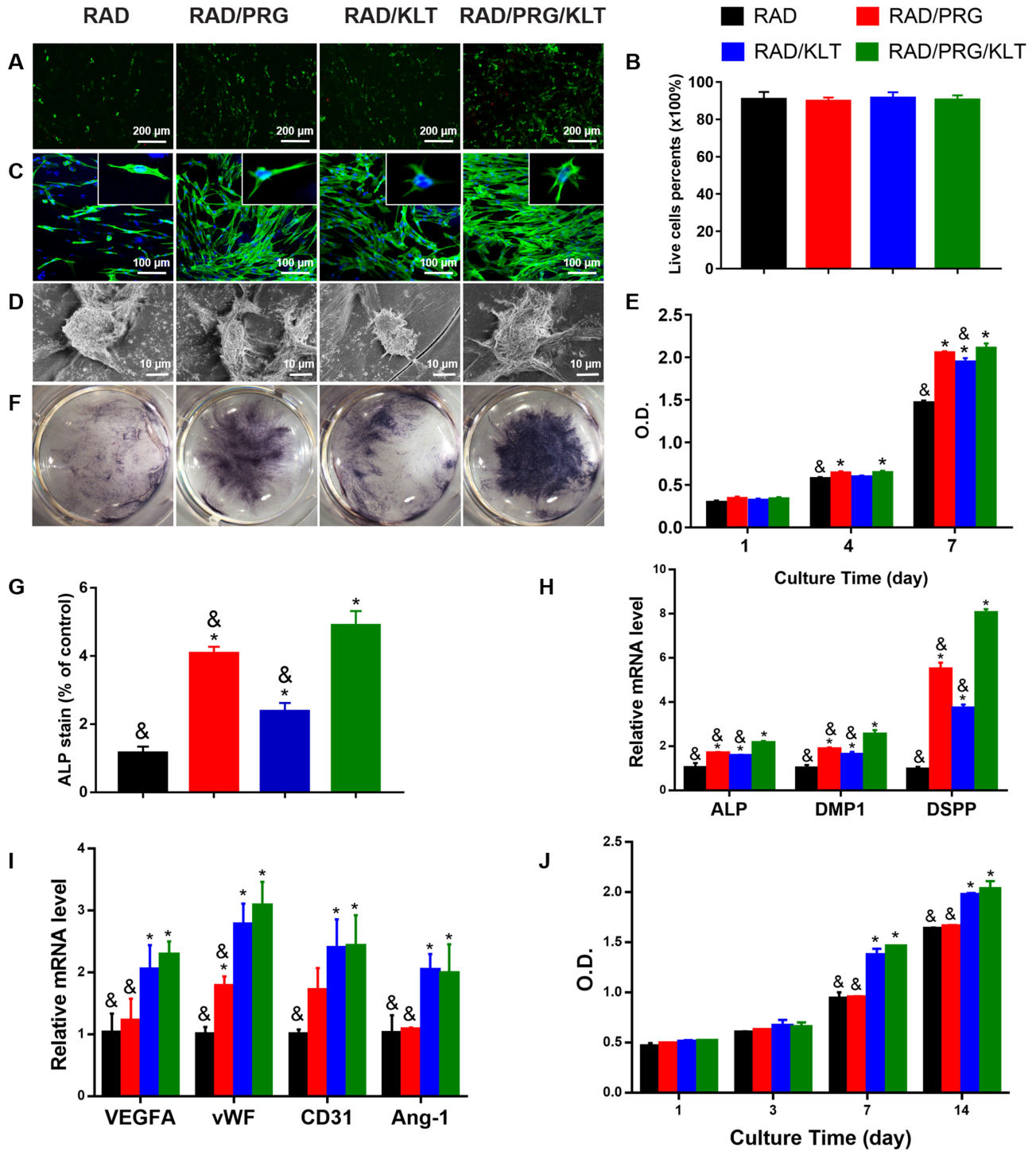

Figure 3 Effects of the SAPs on hDPSCs. (**A**) Live/dead cell viability assay of hDPSCs 3D-cultured in SAPs for 7 days. (**B**) Quantification of the survival rates. (**C**) Fluorescence microscopic images of hDPSCs 3D-cultured in SAP hydrogels; green shows F-actin and blue shows nuclei. (**D**) SEM image of hDPSCs 3D-cultured in the SAPs. (**E**) CCK-8-based quantification of the proliferation rates of hDPSCs 3D cultured in SAPs for 1, 4, and 7 days. (**F**) Mineralized nodule formation of hDPSCs 3D cultured in the SAPs for 14 days shown using ALP staining. (**G**) Quantification of ALP staining. (**H**) Quantification of the levels of gene expression in hDPSCs 3D-cultured in the SAPs after 14 days of odontogenic induction using RT-qPCR. (**I**) Quantification of the levels of gene expression in hDPSCs 3D-cultured in the SAPs for 14 days using RT-qPCR. (**J**) VEGF-secretory abilities of hDPSCs 3D-cultured in SAPs for 1, 3, 7, and 14 days; as determined using ELISA assays. The following symbols indicate significant differences ($P < 0.05$): *Compared to RAD; &Compared to RAD/PRG/KLT.

The ratios of the coronal pulp, the thickness and the porosity of the regenerated dental bridges were measured to further quantify the histology of the regenerative tissues. A higher ratio of the coronal pulp was observed in the RAD/PRG/KLT group than in the other groups (Figure 5H), and greater thickness of the dental bridges in functionalized SAP groups, but no

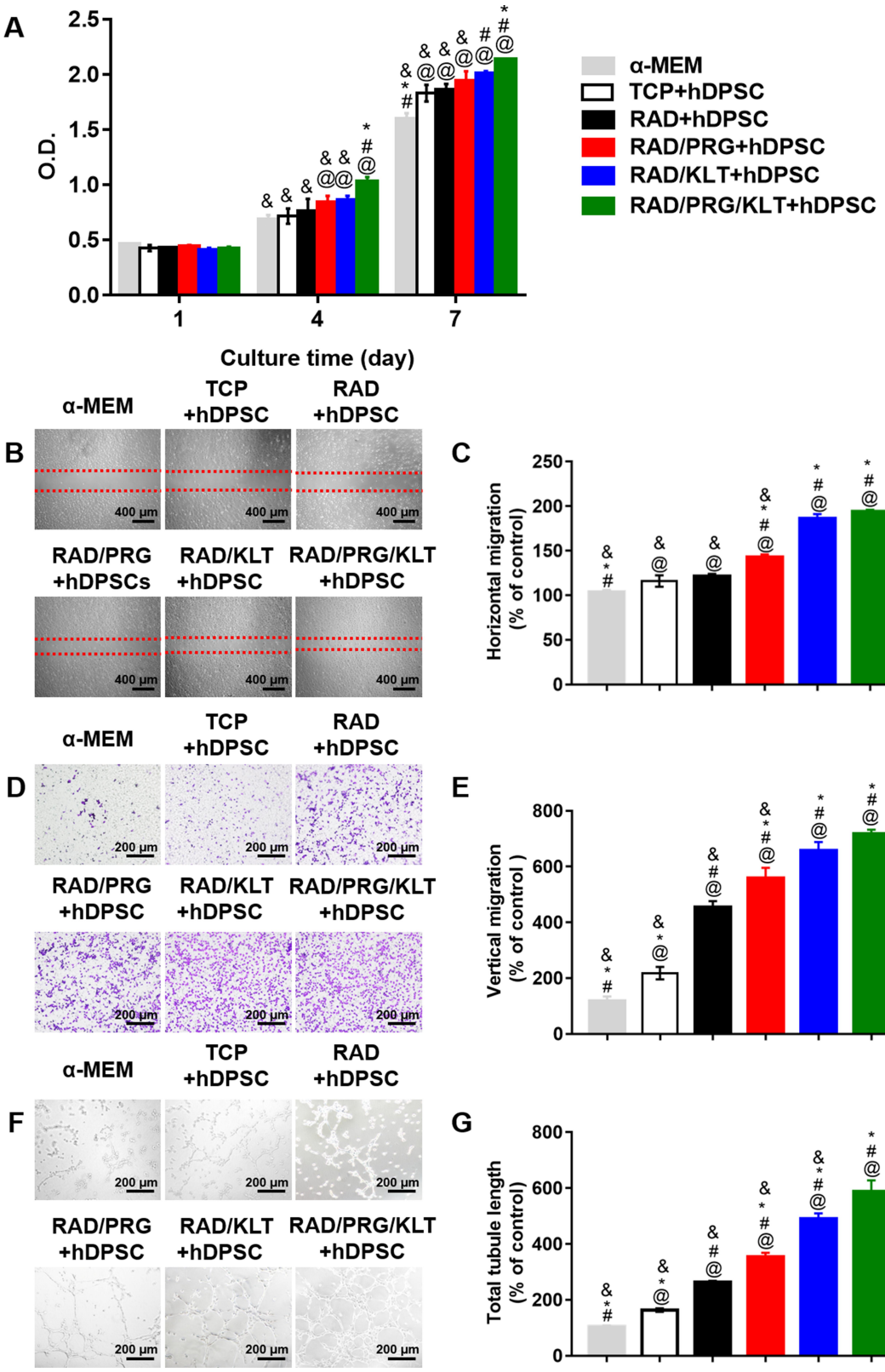

Figure 4 Effects of hDPSCs/SAPs on HUVECs. (**A**) CCK-8-based quantification of the proliferation rates of HUVECs that were 3D-cultured the SAP scaffolds for 1, 4, and 7 days. (**B**) Horizontal migration of HUVECs. (**C**) Quantification of the horizontal migration of HUVECs in CM. (**D**) Vertical migration of HUVECs. (**E**) Quantification of the vertical migration of HUVECs to CM. (**F**) Tube formation of HUVECs. (**G**) Quantification of tube formation. The following symbols indicate significant differences ($P < 0.05$): $^{@}$Compared to α-MEM; $^{\#}$Compared to TCP; *Compared to RAD; $^{\&}$Compared to RAD/PRG/KLT.

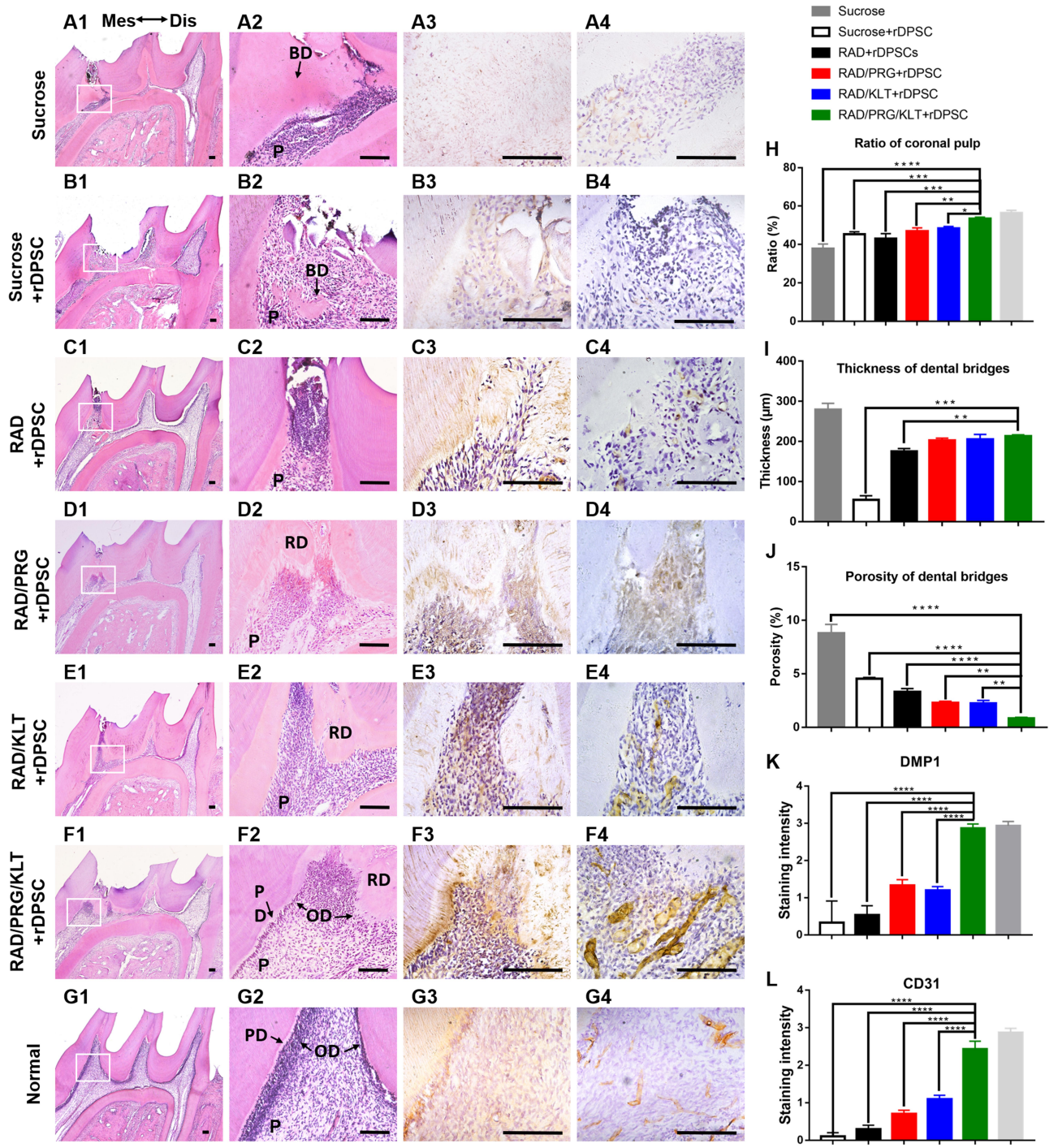

Figure 5 Effects of rDPSCs/SAPs in a partially pulpotomized rat molar model. (**A1–G1**) Sagittal views of a rat upper first molar 28 days after treatment. (**A2–G2**) High-magnification views of the boxed areas in panels A1-G1. (**A3–G3**) IHC staining of DMP1 in groups (**A1–G1**). (**A4–G4**) IHC staining of CD31 in groups (**A1–G1**). (**H**) Quantification of the ratio of coronal pulp. (**I**) Quantification of the thickness of dental bridges. (**J**) Quantification of the porosity of dental bridges. (**K**) Staining intensity of the IHC sample for DMP1. (**L**) Staining intensity of the IHC sample for CD31. Bars = 100 μm. *P < 0.05; **P < 0.01; ***P< 0.001; ****P< 0.0001.
Abbreviations: BD, bone-like dentin; Dis, distal side; Mes, mesial side; OD, odontoblast-like cells; P, pulp; PD, predentin; RD, reparative dentin.

obvious differences were detected between these functionalized SAP groups (P>0.05) (Figure 5I). While the porosity of dental bridges was lower in RAD/PRG/KLT group than in the other groups (P<0.05) (Figure 5J).

In the sucrose+rDPSC group, IHC staining for DMP1 or CD31 was not observed. The IHC staining intensities of DMP1 and CD31 were significantly stronger around the newly formed hard tissue area in the RAD/PRG/KLT

+rDPSC group than in the RAD+rDPSC, RAD/PRG+rDPSC and RAD/KLT+rDPSC groups (P<0.01) (Figure 5H and I).

Discussion

In this study, we hypothesized that SAP-based biomimetic scaffolds created using a single-step preparation that not only exhibited injectability and a 3D nanofibrous structure but also promoted adequate attachment and angiogenesis would be a good choice for dental pulp tissue engineering during DPC regeneration.[37] Here, we designed a simple single-step strategy and one-pot synthesis procedure that addressed all of these considerations. We then examined whether a combination of a cell adhesion-promoting SAP (RAD/PRG) and an angiogenic SAP (RAD/KLT) successfully modulated both odontogenesis and vascularization during DPC regeneration. Based on our findings, the RAD hydrogel modified with PRG and KLT significantly improved the proliferation rate and VEGF-secreting capability of hDPSCs. Furthermore, the CM from RAD/PRG/KLT resulted in an increased cell proliferation rate and enhanced tube formation in HUVECs. Moreover, animal studies using a partially pulpotomized rat molar model revealed that the RAD/PRG/KLT scaffold effectively induced the formation of DPC analogous to the natural tooth structure.

This article represents the first report evaluating a multifunctionalized SAP scaffold for DPC regeneration. Our SAP-based scaffold system is injectable, provides a 3D cell culture environment for DPSCs, mimics the ECM of dental pulp, and combines multiple functional motifs and the slow release of GFs. Our study is the first to apply a scaffold with a cell adhesion-inducing motif and vascularization motif together to induce pulp regeneration. Other studies have focused on integrin-specific hydrogels functionalized with VEGF for vascularization,[38,39] FGF-2 and VEGF functionalization of hydrogels to modulate angiogenesis.[40] In our study, these two motifs concurrently promoted adequate attachment, rapid vascularization and appropriate mineralization during DPC regeneration.

Biomimetic scaffolds have been developed to regulate the local microenvironment and promote stem cell survival and differentiation in tissue engineering.[41] Among these scaffolds, the hydrogel not only exhibits good biocompatibility, biodegradability and the ability to offer 3D porous network, but also is able to carry various kinds of bioactive agents.[42] From a translational perspective, synthetic materials for SAP-based scaffolds composed of natural amino acids are able to be mechanically tuned and biologically functionalized to protect transplanted DPSCs and to promote their attachment, proliferation, and differentiation.[14,43] Based on accumulating evidence, the ideal scaffold should be injectable to allow it to conform to the variable shapes of pulp chambers.[29] Uniquely, RAD is a SAP hydrogel composed of a 16 residue peptide in aqueous solutions that rapidly produces novel supramolecular architectures with structures similar to the natural ECM. It is potentially able to be poured into a pulp chamber, and cells subsequently migrate and proliferate within the peptide hydrogel. Furthermore, when RAD was initially used in stem cell-based regenerative endodontics, DPSCs in RAD exhibited cytoplasmic elongation and expressed DMP-1 and DSPP.[29] In addition, constructs with stem cells plus RAD significantly accelerate the formation of dentin bridges,[44] pulp-like tissues with odontoblasts[30] and capillaries.[45] Moreover, a combination of VEGF-overexpressing and SDF-1α-overexpressing DPSCs encapsulated in RAD increases the area of vascularized and regenerating dental pulp in vivo.[22] A construct built using newborn mouse molar crowns with RAD without the use of exogenous GFs led to the formation of viable vascularized tissue and odontoblast-like cells.[46] Last but not least, in recent years, SAP-based hydrogels have been subjected to clinical trials or have reached the clinical market.[47,48] According to the studies referenced above, RAD has been used successfully in regenerative endodontics as a liquid that is injected and conforms to the variable shapes of pulp chambers. These studies prompted us to exploit RAD as a backbone for designing an ideal scaffold for DPC regeneration.

The second structure tested using CD and FTIR and the microstructure observed using AFM suggested that the functionalized motifs were incorporated into the backbone RAD quite well in the functionalized peptide mixtures. These results were further verified by an SEM analysis after DPSC encapsulation and gelation of the SAPs. Additionally, these nanofibrous 3D structures were significantly smaller than hDPSCs and provide an ECM-like microenvironment for these cells. Furthermore, the single-step cell encapsulation and bioactive peptide tethering strategy enabled the rapid, efficient and reproducible production of cell-hydrogel constructs. Notably, this versatile strategy eliminated the poisonous chemical functionalization and purification steps that are required in other tethering protocols. As shown in our study, the SAP-based platform—RAD/PRG/KLT hydrogel supported DPSC differentiation toward odontogenic and angiogenic phenotypes in the 3D culture environment, even in the absence of additional adhesion proteins and GFs, except for those

functional motifs in the cell media. In this study, our SAP-based platform served as the 3D culture environment for DPSCs, and the functional motifs present on the nanofiber surfaces surrounded DPSCs in all dimensions, thus providing an appropriate environment that was similar to native dental pulp. Specifically, the functional motif PRG mimics the fibronectin in the ECM and targets integrins on DPSCs, while the functional motif KLT simulates the growth factor VEGF and targets VEGFR on DPSCs.

The SAP-based scaffold has been applied in regenerative medicine, such as spinal cord regeneration, bone regeneration, and the formation of blood vessels in arterial disease and cardiovascular diseases. It has been functionalized with multiple bioactive peptides according to the regeneration requirements of the target tissue. A class of functionalized peptides designed for the 3D culture of mouse adult neural stem cells was prepared by linking different bioactive motifs to RADA16-I. A scaffold containing the bone marrow homing motifs BMHP1 and BMHP2 significantly promotes neural cell survival without assistance of additional soluble GFs.[49] The proangiogenic potential of the RAD/PRG and RAD/KLT nanofiber scaffolds was established by Liu et al The scaffolds significantly promoted endothelial cell growth, migration and tubulogenesis in vitro.[50] Horii et al designed three peptide scaffolds derived from osteogenic growth peptide (ALK), the cell adhesion domain of osteopontin (DGR) and 2-unit RGD motifs (PRG) for osteoblasts.[17] These peptide scaffolds promoted the proliferation, differentiation and migration of the mouse pre-osteoblast MC3T3-E1. In the present study, we observed a significant increase in the proliferation rate of the RAD/PRG/KLT group. A potential explanation for this finding is the presence of the PRG sequences, which are cell-binding domains recognized by approximately half of the more than 20 known α/β integrins and promote the proliferation of many cell types.[51,52] Consistent with our results, studies of the role of PRG in RAD have reported that inclusion of the osteopontin cell adhesion motif PGR and the osteogenic growth peptide ALK in RAD mixtures stimulate cell migration and promote proliferation and osteogenic differentiation.[17] Similar results were obtained in terms of bone-healing ability and periodontal ligament tissue regeneration. PRG and other peptides induced good cell adhesion, proliferation and differentiation.[26,53]

RAD/PRG/KLT clearly plays a consistent role of promoting proliferation and vascularization during odontogenesis. This finding is consistent with the results of other studies showing that both PRG and KLT promote proliferation and osteogenic differentiation during osteogenesis. The angiogenic activity of the two functional motifs, PRG and KLT, in RAD was systematically studied using the chicken embryo chorioallantoic membrane assay, and the results suggested that the functionalized peptide scaffolds had satisfactory angiogenic properties.[54] RAD peptide scaffolds functionalized with RAD/PRG or RAD/KLT improved the localization, survival and therapeutic effects of bone marrow-derived stromal cells and showed promising potential for the treatment of acute myocardial infarction.[55] Both the RAD/KLT and RAD/PRG/KLT scaffolds showed statistically significant increases in VEGF concentrations and HUVEC activity compared to pure RAD scaffolds alone. The variations between scaffolds increased 7 days later, suggesting that the effect of functional scaffolds appears to be more important in the later stage of differentiation. According to previous studies, DPSCs have the capacity to differentiate into the endothelial cell lineage. On the other hand, DPSCs also possess a proangiogenic property because they secrete VEGF and other pro-angiogenic factors.[56] In future studies, we should employ additional markers and methods to support the former conclusion.

Notably, our animal studies identified the RAD/PRG/KLT hydrogel as exerting a superior effect on the formation of DPC with a structure analogous to natural teeth. Transplantation of a combination of culture-expanded rDPSCs in the RAD/PRG/KLT hydrogel resulted in a significantly increased number of intact dentin bridges and well-aligned odontoblast-like cell layers over the course of a 28-day observation period. Notably, the dentin bridge formed with an appropriate thickness and the "pulp horn" architecture similar to natural teeth, which reserves sufficient space for the regeneration of pulp tissue. A potential explanation for this result is that our design combining the PRG and KLT motifs in RAD achieved an orderly and coordinated symbiosis of pulp tissue regeneration, vascularization and mineralization.

Further in vivo studies of large animal models, such as pigs or dogs, are needed to support our results. The delivery of anti-inflammatory drugs using the SAP scaffold should be considered and requires further investigation.

Conclusions

In conclusion, RAD/PRG/KLT can promote the survival and differentiation of DPSCs to promote DPC regeneration in partially pulpotomized rat molars over the course of a 28-

day period. Our findings demonstrate the significance of creating a microenvironment that supports stem cell adhesion and angiogenesis, which contributes to the creation of an optimal environment for dental pulp regeneration.

Acknowledgments

The work was supported by National Natural Science Foundation of China (grant numbers 81870760, 81570966); Fundamental Research Funds for the Central Universities (grant number 22120190217); Wenzhou Municipal Science and Technology Bureau Foundation (grant number Y20190490); and Zhejiang Provincial Natural Science Foundation of China (grant number LY19H140004).

Author Contributions

Kun Xia and Zhuo Chen contributed to conception, design, data acquisition, and interpretation, drafted and critically revised the manuscript. Jie Chen, Huaxing Xu, Yunfei Xu, Ting Yang contributed to conception, design and critically revised the manuscript. Qi Zhang contributed to conception, design, data analysis, and critically revised the manuscript. All authors gave final approval and agree to be accountable for all aspects of the work.

Disclosure

The authors report no conflicts of interest for this work.

References

1. Fawzy El-Sayed KM, Ahmed GM, Abouauf EA, Schwendicke F. Stem/progenitor cell-mediated pulpal tissue regeneration: a systematic review and meta-analysis. *Int Endod J*. 2019;52(11):1573–1585. doi:10.1111/iej.13177
2. Albuquerque MT, Valera MC, Nakashima M, Nor JE, Bottino MC. Tissue-engineering-based strategies for regenerative endodontics. *J Dent Res*. 2014;93(12):1222–1231. doi:10.1177/0022034514549809
3. Lutolf MP, Gilbert PM, Blau HM. Designing materials to direct stem-cell fate. *Nature*. 2009;462(7272):433–441. doi:10.1038/nature08602
4. Piva E, Silva AF, Nor JE. Functionalized scaffolds to control dental pulp stem cell fate. *J Endod*. 2014;40(4 Suppl):S33–40. doi:10.1016/j.joen.2014.01.013
5. Moussa DG, Aparicio C. Present and future of tissue engineering scaffolds for dentin-pulp complex regeneration. *J Tissue Eng Regen Med*. 2019;13(1):58–75. doi:10.1002/term.2769
6. Ravindran S, Zhang Y, Huang CC, George A. Odontogenic induction of dental stem cells by extracellular matrix-inspired three-dimensional scaffold. *Tissue Eng Part A*. 2014;20(1–2):92–102. doi:10.1089/ten.tea.2013.0192
7. Song JS, Takimoto K, Jeon M, Vadakekalam J, Ruparel NB, Diogenes A. Decellularized human dental pulp as a scaffold for regenerative endodontics. *J Dent Res*. 2017;96(6):640–646. doi:10.1177/0022034517693606
8. Zhang X, Li H, Sun J, et al. Cell-derived micro-environment helps dental pulp stem cells promote dental pulp regeneration. *Cell Prolif*. 2017;50(5):e12361. doi:10.1111/cpr.12361
9. Rubert Perez CM, Stephanopoulos N, Sur S, Lee SS, Newcomb C, Stupp SI. The powerful functions of peptide-based bioactive matrices for regenerative medicine. *Ann Biomed Eng*. 2015;43(3):501–514. doi:10.1007/s10439-014-1166-6
10. Sargeant TD, Aparicio C, Goldberger JE, Cui H, Stupp SI. Mineralization of peptide amphiphile nanofibers and its effect on the differentiation of human mesenchymal stem cells. *Acta Biomater*. 2012;8(7):2456–2465. doi:10.1016/j.actbio.2012.03.026
11. Holmes TC, de Lacalle S, Su X, Liu G, Rich A, Zhang S. Extensive neurite outgrowth and active synapse formation on self-assembling peptide scaffolds. *Proc Natl Acad Sci U S A*. 2000;97(12):6728–6733. doi:10.1073/pnas.97.12.6728
12. Lutolf MP, Hubbell JA. Synthetic biomaterials as instructive extracellular microenvironments for morphogenesis in tissue engineering. *Nat Biotechnol*. 2005;23(1):47–55. doi:10.1038/nbt1055
13. Dou XQ, Feng CL. Amino acids and peptide-based supramolecular hydrogels for three-dimensional cell culture. *Adv Mater*. 2017;29(16):1604062. doi:10.1002/adma.201604062
14. Pugliese R, Gelain F. Peptidic biomaterials: from self-assembling to regenerative medicine. *Trends Biotechnol*. 2017;35(2):145–158. doi:10.1016/j.tibtech.2016.09.004
15. Lu J, Yan X, Sun X, et al. Synergistic effects of dual-presenting VEGF- and BDNF-mimetic peptide epitopes from self-assembling peptide hydrogels on peripheral nerve regeneration. *Nanoscale*. 2019;11(42):19943–19958. doi:10.1039/C9NR04521J
16. Sun Y, Li W, Wu X, et al. Functional self-assembling peptide nanofiber hydrogels designed for nerve degeneration. *ACS Appl Mater Interfaces*. 2016;8(3):2348–2359. doi:10.1021/acsami.5b11473
17. Horii A, Wang X, Gelain F, Zhang S, Isalan M. Biological designer self-assembling peptide nanofiber scaffolds significantly enhance osteoblast proliferation, differentiation and 3-D migration. *PLoS One*. 2007;2(2):e190. doi:10.1371/journal.pone.0000190
18. Kisiday J, Jin M, Kurz B, et al. Self-assembling peptide hydrogel fosters chondrocyte extracellular matrix production and cell division: implications for cartilage tissue repair. *Proc Natl Acad Sci U S A*. 2002;99(15):9996–10001. doi:10.1073/pnas.142309999
19. Suzuki T, Lee CH, Chen M, et al. Induced migration of dental pulp stem cells for in vivo pulp regeneration. *J Dent Res*. 2011;90(8):1013–1018. doi:10.1177/0022034511408426
20. Casagrande L, Demarco FF, Zhang Z, Araujo FB, Shi S, Nor JE. Dentin-derived BMP-2 and odontoblast differentiation. *J Dent Res*. 2010;89(6):603–608. doi:10.1177/0022034510364487
21. Wu S, Zhou Y, Yu Y, et al. Evaluation of chitosan hydrogel for sustained delivery of VEGF for odontogenic differentiation of dental pulp stem cells. *Stem Cells Int*. 2019;2019:1515040.
22. Zhu L, Dissanayaka WL, Zhang C. Dental pulp stem cells overexpressing stromal-derived factor-1alpha and vascular endothelial growth factor in dental pulp regeneration. *Clin Oral Investig*. 2019;23(5):2497–2509. doi:10.1007/s00784-018-2699-0
23. Tessmar JK, Gopferich AM. Matrices and scaffolds for protein delivery in tissue engineering. *Adv Drug Deliv Rev*. 2007;59(4–5):274–-291. doi:10.1016/j.addr.2007.03.020
24. Galler KM, D'Souza RN, Hartgerink JD, Schmalz G. Scaffolds for dental pulp tissue engineering. *Adv Dent Res*. 2011;23(3):333–339. doi:10.1177/0022034511405326
25. Tao H, Wu Y, Li H, et al. BMP7-based functionalized self-assembling peptides for nucleus pulposus tissue engineering. *ACS Appl Mater Interfaces*. 2015;7(31):17076–17087. doi:10.1021/acsami.5b03605
26. Kumada Y, Zhang S, Orgel JPRO. Significant type I and type III collagen production from human periodontal ligament fibroblasts in 3D peptide scaffolds without extra growth factors. *PLoS One*. 2010;5(4):e10305. doi:10.1371/journal.pone.0010305

27. D'Andrea LD, Iaccarino G, Fattorusso R, et al. Targeting angiogenesis: structural characterization and biological properties of a de novo engineered VEGF mimicking peptide. *Proc Natl Acad Sci U S A*. 2005;102(40):14215–14220. doi:10.1073/pnas.0505047102
28. Finetti F, Basile A, Capasso D, et al. Functional and pharmacological characterization of a VEGF mimetic peptide on reparative angiogenesis. *Biochem Pharmacol*. 2012;84(3):303–311. doi:10.1016/j.bcp.2012.04.011
29. Cavalcanti BN, Zeitlin BD, Nor JE. A hydrogel scaffold that maintains viability and supports differentiation of dental pulp stem cells. *Dent Mater*. 2013;29(1):97–102. doi:10.1016/j.dental.2012.08.002
30. Rosa V, Zhang Z, Grande RH, Nor JE. Dental pulp tissue engineering in full-length human root canals. *J Dent Res*. 2013;92(11):970–975. doi:10.1177/0022034513505772
31. Chan KH, Lee WH, Ni M, Loo Y, Hauser CAE. C-terminal residue of ultrashort peptides impacts on molecular self-assembly, hydrogelation, and interaction with small-molecule drugs. *Sci Rep*. 2018;8(1):17127. doi:10.1038/s41598-018-35431-2
32. Chan KH, Xue B, Robinson RC, Hauser CAE. Systematic moiety variations of ultrashort peptides produce profound effects on self-assembly, nanostructure formation, hydrogelation, and phase transition. *Sci Rep*. 2017;7(1):12897. doi:10.1038/s41598-017-12694-9
33. Mishra A, Chan K-H, Reithofer MR, Hauser CAE. Influence of metal salts on the hydrogelation properties of ultrashort aliphatic peptides. *RSC Adv*. 2013;3(25):9985. doi:10.1039/c3ra40598b
34. Dissanayaka WL, Zhu X, Zhang C, Jin L. Characterization of dental pulp stem cells isolated from canine premolars. *J Endod*. 2011;37(8):1074–1080. doi:10.1016/j.joen.2011.04.004
35. Koliniotou-Koumpia E, Tziafas D. Pulpal responses following direct pulp capping of healthy dog teeth with dentine adhesive systems. *J Dent*. 2005;33(8):639–647. doi:10.1016/j.jdent.2004.12.007
36. Liu Y, Du H, Wang Y, et al. Osteoprotegerin-knockout mice developed early onset root resorption. *J Endod*. 2016;42(10):1516–1522. doi:10.1016/j.joen.2016.07.008
37. Gong T, Heng BC, Lo EC, Zhang C. Current advance and future prospects of tissue engineering approach to dentin/pulp regenerative therapy. *Stem Cells Int*. 2016;2016:9204574. doi:10.1155/2016/9204574
38. Lee SI, Lee ES, El-Fiqi A, Lee SY, Eun-Cheol K, Kim HW. Stimulation of odontogenesis and angiogenesis via bioactive nanocomposite calcium phosphate cements through integrin and VEGF signaling pathways. *J Biomed Nanotechnol*. 2016;12(5):1048–1062. doi:10.1166/jbn.2016.2209
39. Garcia JR, Clark AY, Garcia AJ. Integrin-specific hydrogels functionalized with VEGF for vascularization and bone regeneration of critical-size bone defects. *J Biomed Mater Res A*. 2016;104(4):889–900. doi:10.1002/jbm.a.35626
40. Zieris A, Prokoph S, Levental KR, et al. FGF-2 and VEGF functionalization of starPEG-heparin hydrogels to modulate biomolecular and physical cues of angiogenesis. *Biomaterials*. 2010;31(31):7985–7994. doi:10.1016/j.biomaterials.2010.07.021
41. Huang K, Hou J, Gu Z, Wu J. Egg-white-/eggshell-based biomimetic hybrid hydrogels for bone regeneration. *ACS Biomater Sci Eng*. 2019;5(10):5384–5391. doi:10.1021/acsbiomaterials.9b00990
42. Zhou Y, Gu Z, Liu J, Huang K, Liu G, Wu J. Arginine based poly (ester amide)/hyaluronic acid hybrid hydrogels for bone tissue engineering. *Carbohydr Polym*. 2020;230:115640. doi:10.1016/j.carbpol.2019.115640
43. Hauser CA, Zhang S. Designer self-assembling peptide nanofiber biological materials. *Chem Soc Rev*. 2010;39(8):2780–2790. doi:10.1039/b921448h
44. Bykova NI, Sirak SV, Kobylkina TL, Odolsky AV, Bykov IM, Arutyunov AV. [Optimization of reparative dentinogenesis in experimental osteoporosis]. Article in Russion. *Stomatologiia*. 2017;96(6):4–8. doi:10.17116/stomat20179664-8
45. Chan B, Wong RW, Rabie B. In vivo production of mineralised tissue pieces for clinical use: a qualitative pilot study using human dental pulp cell. *Int J Oral Maxillofac Surg*. 2011;40(6):612–620. doi:10.1016/j.ijom.2011.01.008
46. Pelissari C, Paris AFC, Mantesso A, Trierveiler M. Apical papilla cells are capable of forming a pulplike tissue with odontoblastlike cells without the use of exogenous growth factors. *J Endod*. 2018;44(11):1671–1676. doi:10.1016/j.joen.2018.08.005
47. Yoshida M, Goto N, Kawaguchi M, et al. Initial clinical trial of a novel hemostat, TDM-621, in the endoscopic treatments of the gastric tumors. *J Gastroenterol Hepatol*. 2014;29(Suppl 4):77–79. doi:10.1111/jgh.12798
48. Masuhara H, Fujii T, Watanabe Y, Koyama N, Tokuhiro K. Novel infectious agent-free hemostatic material (TDM-621) in cardiovascular surgery. *Ann Thorac Cardiovasc Surg*. 2012;18(5):444–451. doi:10.5761/atcs.oa.12.01977
49. Gelain F, Bottai D, Vescovi A, Zhang S, Herman C. Designer self-assembling peptide nanofiber scaffolds for adult mouse neural stem cell 3-dimensional cultures. *PLoS One*. 2006;1:e119. doi:10.1371/journal.pone.0000119
50. Liu X, Wang X, Wang X, et al. Functionalized self-assembling peptide nanofiber hydrogels mimic stem cell niche to control human adipose stem cell behavior in vitro. *Acta Biomater*. 2013;9(6):6798–6805. doi:10.1016/j.actbio.2013.01.027
51. Hersel U, Dahmen C, Kessler H. RGD modified polymers: biomaterials for stimulated cell adhesion and beyond. *Biomaterials*. 2003;24(24):4385–4415. doi:10.1016/S0142-9612(03)00343-0
52. Ruoslahti E. RGD and other recognition sequences for integrins. *Annu Rev Cell Dev Biol*. 1996;12:697–715. doi:10.1146/annurev.cellbio.12.1.697
53. Gogoi S, Maji S, Mishra D, Devi KS, Maiti TK, Karak N. Nano-bio engineered carbon dot-peptide functionalized water dispersible hyperbranched polyurethane for bone tissue regeneration. *Macromol Biosci*. 2017;17:3. doi:10.1002/mabi.201600271
54. Liu X, Wang X, Horii A, et al. In vivo studies on angiogenic activity of two designer self-assembling peptide scaffold hydrogels in the chicken embryo chorioallantoic membrane. *Nanoscale*. 2012;4(8):2720–2727. doi:10.1039/c2nr00001f
55. Li X, Chen YY, Wang XM, et al. Image-guided stem cells with functionalized self-assembling peptide nanofibers for treatment of acute myocardial infarction in a mouse model. *Am J Transl Res*. 2017;9(8):3723–3731.
56. Dissanayaka WL, Zhang C. The role of vasculature engineering in dental pulp regeneration. *J Endod*. 2017;43(9s):S102–s106. doi:10.1016/j.joen.2017.09.003

International Journal of Nanomedicine

Dovepress

Publish your work in this journal

The International Journal of Nanomedicine is an international, peer-reviewed journal focusing on the application of nanotechnology in diagnostics, therapeutics, and drug delivery systems throughout the biomedical field. This journal is indexed on PubMed Central, MedLine, CAS, SciSearch®, Current Contents®/Clinical Medicine, Journal Citation Reports/Science Edition, EMBase, Scopus and the Elsevier Bibliographic databases. The manuscript management system is completely online and includes a very quick and fair peer-review system, which is all easy to use. Visit http://www.dovepress.com/testimonials.php to read real quotes from published authors.

Submit your manuscript here: https://www.dovepress.com/international-journal-of-nanomedicine-journal